Journal of Luminescence 251 (2022) 119147

Contents lists available at ScienceDirect

Journal of Luminescence

journal homepage: www.elsevier.com/locate/jlumin

Full Length Article

Elimination of unexpected destruction on $CsPbBr_xI_{3-x}$ nanocrystals arising from polymer matrix

Yajie Zhu [a,1], Daocheng Hong [a,b,1], Yan Nie [a,1], Hanyu Liu [a], Sushu Wan [a], Mingcai Xie [a], Weiqing Yang [a], Zhihong Wei [a], Siyang Ye [a], Yuxi Tian [a,*]

[a] Laboratory of Mesoscopic Chemistry of MOE, School of Chemistry and Chemical Engineering, Nanjing University, Nanjing, Jiangsu, 210023, China
[b] Key Laboratory for Advanced Technology in Environmental Protection of Jiangsu Province, Yancheng Institute of Technology, Yancheng, Jiangsu, 224051, China

A B S T R A C T

Cesium lead halide perovskite ($CsPbX_3$) nanocrystals (NCs) have exhibited promising applications in light-emitting diodes (LEDs) due to their tunable bandgap and high quantum efficiency. Backlighting LEDs based on $CsPbBr_3$ NCs with green emission have been widely designed to show their superiority. However, unlike $CsPbBr_3$ NCs, backlighting LEDs composed of mixed-halide perovskite ($CsPbBr_xI_{3-x}$) NCs have rarely been reported and should be further applied in colorful LEDs for granted, mainly because of the unexpected destructive effects from the commercial polymer matrix verified in this work. Purification of a commercial polymer matrix was promoted as an effective method to eliminate the destructive effects. Further investigation proved that the species with strong polarity and oxidability, e.g., BPO in commercial PMMA, are responsible for such destructive effects by inducing the structural transformation of $CsPbBr_xI_{3-x}$ NCs. We believe such results can help to gain a deeper understanding of the degradation mechanism of mixed-halide perovskite materials and indicate a promising method to develop stable colorful perovskite-based LEDs.

1. Introduction

All-inorganic cesium lead halide perovskite ($CsPbX_3$, X = Cl, Br, I) NCs show outstanding optical properties, such as high photoluminescence quantum yields (PLQYs, up to 90%), narrow emission peak bandwidths (<50 nm), and favorable optical gains with low-threshold emission. [1] In addition, a facile fabrication method [2] and spectrally tunable emission [3,4] simply via composition adjustments further extended their attraction. All these advantages make $CsPbX_3$ NCs attractive materials for applications such as light emitting diodes, lasers, and photodetectors. [4–8] In particular, optoelectronic devices based on $CsPbX_3$ QDs have been widely developed. [2,9–11] LEDs based on anion exchange of $CsPbBr_3$ NCs exhibit excellent EQEs over 20%. [12]

Although $CsPbX_3$ (X = Br, I) perovskite NCs have been widely recognized, there are few reports about the fabrication of optoelectronic devices using mixed-halide inorganic perovskite nanocrystals. This could be due to its intrinsic chemical instability, which limits all technological applications. When $CsPbX_3$ perovskite NCs are processed into a composite or a layer, where they are exposed to humidity, light, temperature and so on, they rapidly degrade. This is associated with highly dynamic ligand binding to the NCs surface. [13] Moreover, the fast anion-exchange reaction between different halide perovskite NCs brings many difficulties, [14] leading to an impediment to further functionalization. One of the recognized methods for stabilizing lead halide perovskite NCs for lighting applications is embedding the NCs into a polymeric matrix such as PMMA. [15–17] PMMA not only improves the stability of perovskite QDs but also endows perovskites with advantages in many aspects, such as mechanical performance and enhanced luminescent properties. [11,18,19] Zhu et al. constructed green light-emitting $CsPbBr_3$@PMMA composites through a hot-injection method, which exhibited a high PLQY of 72% and good stability in water. [20] Xin et al. integrated the formation of $CsPbBr_3$ crystals and PMMA in a one-pot reaction, and then a white LED device successfully based on green emissive perovskite−polymer composites mixed with red emissive rare-earth phosphors was fabricated with feasible color characteristics and narrow bandwidths. [21] However, such a protection effect of a commercial polymer matrix (e.g., PMMA) on $CsPbBr_3$ NCs [22,23] has not been reported for mixed-halide perovskite NCs with tunable PL emission.

Here, in this work, considering the successful application of PMMA in $CsPbBr_3$ NCs, we speculated that PMMA can also effectively enhance the stability of mixed-halide $CsPbBr_xI_{3-x}$ NCs and block halide exchange effects during the process of $CsPbBr_xI_{3-x}$ NCs. However, after we

* Corresponding author.
E-mail address: tyx@nju.edu.cn (Y. Tian).
[1] These authors contributed equally.

https://doi.org/10.1016/j.jlumin.2022.119147
Received 22 March 2022; Received in revised form 8 July 2022; Accepted 18 July 2022
Available online 21 July 2022

synthesized mixed-halide $CsPbBr_xI_{3-x}$ NCs and embedded them into PMMA to realize colorful PL emission, contrary to our assumption, PMMA accelerated the degradation of $CsPbBr_xI_{3-x}$ NCs. Further study confirmed that only purified PMMA can be taken as the polymer matrix to improve their PL stability. With TRPL measurements and control experiments, the degradation mechanisms of commercial PMMA were suggested, which provided efficient guidance for constructing optimized perovskite-based LEDs with colorful emission.

2. Experimental methods

2.1. Chemicals and materials

$PbBr_2$, PbI_2, and poly(methyl methacrylate) (PMMA) were purchased from Sigma-Aldrich. Oleylamine (OLA, 80–90%), oleic acid (OA, AR), hexane (GC) and N,N-dimethylformamide (DMF, 99.8%) were purchased from Aladdin. Toluene was purchased from Laibao. Chloroform and acetone (HPLC) were purchased from Sinopharm. CsBr was purchased from p-OLED.

2.2. Synthesis

$CsPbBr_xI_{3-x}$ NCs solution: $CsPbBr_xI_{3-x}$ NCs were prepared following a recrystallization procedure developed by Zeng et al. [24] Take $CsPbBr_2I$ NCs as an example. We prepared a 0.04 M $CsPbBr_2I$ solution first. CsBr (0.1704 g), $PbBr_2$ (0.1468 g), and PbI_2 (0.1844 g) as ion sources were dissolved in DMF (20 ml). OA (100 μl) and OLA (50 μl) as surface ligands were added to the $CsPbBr_2I$ solution (1 ml) to form the precursor solution. The precursor solution was heated at 60° under stirring. Then, a moderate amount of precursor solution was added to toluene under vigorous stirring. Almost immediately, the solutions emitted red light, and $CsPbBr_2I$ NCs were obtained. $CsPbBr_{1.5}I_{1.5}$ NCs and $CsPbBrI_2$ NCs were fabricated in the same way.

$CsPbBr_xI_{3-x}$ NCs film: A $CsPbBr_xI_{3-x}$ NCs film was obtained by dropping the $CsPbBr_xI_{3-x}$ NCs solution onto clean glass cover slips and then annealing at 60 °C for approximately 5 min. The pretreated glass substrates were first treated with 1% Hellmanex III (Hellma) solution and then immersed in an ultrasonic bath to remove the residual substances. Finally, the cover slips were treated by UV irradiation to eliminate the remaining emissive impurities.

2.3. Purification of PMMA

PMMA was dissolved in chloroform with a concentration close to saturation, and then a 6 times larger volume of hexane was added into the polymer solution. With sufficient shaking, the polymer precipitated from the solution. The top solution was poured out. The procedure was repeated three times. The polymer was placed on a heating stage until it dried.

2.4. PL measurements

The PL measurements were taken by a home-built wide-field fluorescence microscope based on Olympus IX73. A 450 nm CW diode laser was used as the excitation light for the sample measurements with a power density of 20 W/cm^2. The fluorescence of the samples was collected by a dry objective lens (Olympus LUCPlanFI 40 ×, NA = 0.6) and detected by an EMCCD camera (iXon Ultra 888, Andor). The PL spectra were measured by putting a transmission grating (Newport, 150 lines/mm) in front of the camera. PL lifetime measurements were performed by using a single-photon counting system (TCSPC, PicoHarp 300) with 450 nm excitation light (5 MHz) from a supercontinuous laser (Fianium SC-400).

3. Results and discussion

To manufacture colorful LEDs with mixed-halide perovskite NCs, we first synthesized $CsPbBr_2I$, $CsPbBr_{1.5}I_{1.5}$ and $CsPbBrI_2$ NCs. Representative TEM images of $CsPbBr_2I$, $CsPbBr_{1.5}I_{1.5}$ and $CsPbBrI_2$ NCs are shown in Fig. 1a, b and 1c, respectively. Compared with the $CsPbBr_3$ NCs [22], the microstructure of $CsPbBr_xI_{3-x}$ NCs deviated from the squares, indicating the effective doping of I^- in $CsPbBr_3$ NCs. The increase in the lattice constants from $CsPbBr_2I$ to $CsPbBrI_2$ can also verify the increase in the iodine content due to the larger ionic radius of I^-. The absorption spectra shown in Fig. 1d presented the bandgaps of $CsPbBr_2I$, $CsPbBr_{1.5}I_{1.5}$ and $CsPbBrI_2$ NCs, which were 2.3 eV, 2.1 eV and 1.9 eV, respectively, coinciding with the PL maxima (552 nm, 606 nm and 647 nm) of the three kinds of NCs. The corresponding XRD peaks (Fig. 1e) at approximately 15.0° and 30.1° prove the formation of the perovskite structure. [25] As the iodine content increased, the shifting of the characteristic peak to small angles corresponds to the variation in the lattice constants from the TEM data. $CsPbBrI_2$ NCs had already partially transformed from the cubic to orthorhombic phase, indicating poor stability. [26]

Then, we characterized the PL properties of $CsPbBr_xI_{3-x}$ NCs solutions treated with and without PMMA. The temporal evolution of the PL spectra from both solutions was monitored in real time via a wide-field fluorescence microscope with continuous excitation at 450 nm under ambient conditions. The $CsPbBr_xI_{3-x}$ NCs solutions with the addition of PMMA were obtained by mixing pristine $CsPbBr_xI_{3-x}$ solutions with 50 g/L PMMA solutions. The pristine $CsPbBr_xI_{3-x}$ NCs solution was also diluted with toluene to maintain the same concentration. From the PL spectra in Fig. 2, a slight blueshift and PL quenching were observed in the pristine $CsPbBr_xI_{3-x}$ solutions, which should result from water and oxygen molecules from air causing decomposition and destruction of their structures [27]. However, unexpectedly destructive effects were observed in the solutions with the addition of PMMA, as shown in Fig. 2d–f. Not only was the PL intensity quenched, but an obvious blueshift of the PL spectrum was also observed within 30 min. The spectral shift can be clearly seen from the colour change of the $CsPbBr_xI_{3-x}$ NCs solutions (Fig. 2 insets).

Because perovskite materials are always vulnerable to oxidizing species, we supposed that there are some similar impurities contained in the purchased PMMA. Thus, we tried to purify the purchased PMMA as depicted in the experimental methods and checked their effect on the stability of $CsPbBr_xI_{3-x}$ NCs, as shown in Figs. S3 and S4. Under continuous illumination, there was a significant enhancement of PL intensity at the beginning. Even though the intensity decreased gradually with time, $CsPbBr_xI_{3-x}$ with purified PMMA still maintained a higher PL intensity than pristine solutions and commercial PMMA-treated solutions throughout the whole process. In addition, the stability of the PL spectra was also greatly improved.

It is worth noting that the $CsPbBr_xI_{3-x}$ NCs mixed with purified PMMA exhibited superior long-term stability. As shown in Fig. 3, the $CsPbBr_xI_{3-x}$ NCs corresponding to different treatments were placed in the dark and monitored for approximately 35 h to compare their PL stability. As a result, the PL spectra of the $CsPbBr_xI_{3-x}$ NCs mixed with commercial PMMA showed a fast blueshift, while pristine $CsPbBr_xI_{3-x}$ NCs solutions exhibited a slower variation in the PL spectra. The PL spectra in the $CsPbBr_xI_{3-x}$ NCs solution treated with purified PMMA were quite stable, especially for $CsPbBrI_2$ NCs. Such results indicate that the purified PMMA polymer can effectively protect the mixed-halide perovskite from degradation. However, it did not completely stop the blueshift of the PL emission, which can be due to the inherent phase instability issues of the $CsPbBr_xI_{3-x}$ NCs resulting from the discrepancy between the mixed halide ions [18,28–31]. Additionally, different preparation methods and environmental conditions during fabrication can also influence the stability of $CsPbBr_xI_{3-x}$ NCs [32,33], indicating that optimized synthesis methods of mixed-halide perovskite NCs can be further developed.

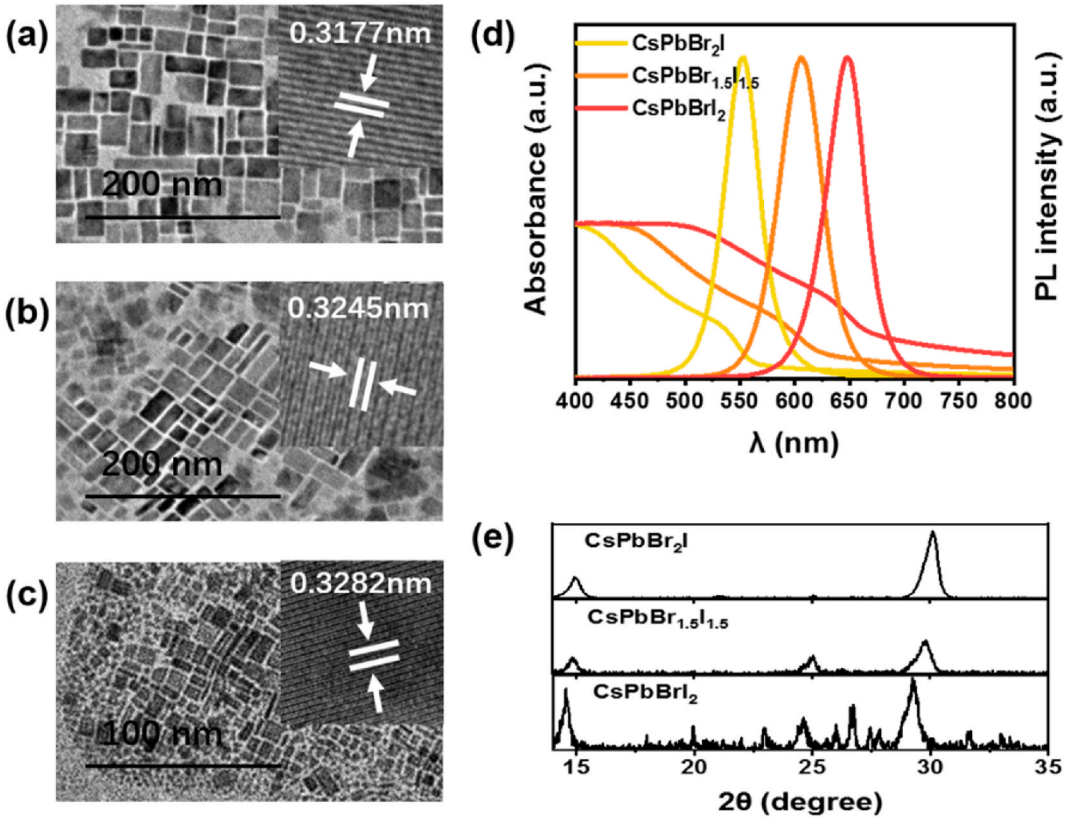

Fig. 1. TEM images of $CsPbBr_2I$ NCs (a), $CsPbBr_{1.5}I_{1.5}$ NCs (b) and $CsPbBrI_2$ NCs (c), and the inset shows the corresponding high-resolution TEM (HRTEM) images. (d) Absorption and photoluminescence spectra of $CsPbBr_2I$, $CsPbBr_{1.5}I_{1.5}$ and $CsPbBrI_2$ NCs. (e) XRD spectra of $CsPbBr_2I$, $CsPbBr_{1.5}I_{1.5}$ and $CsPbBrI_2$ NCs.

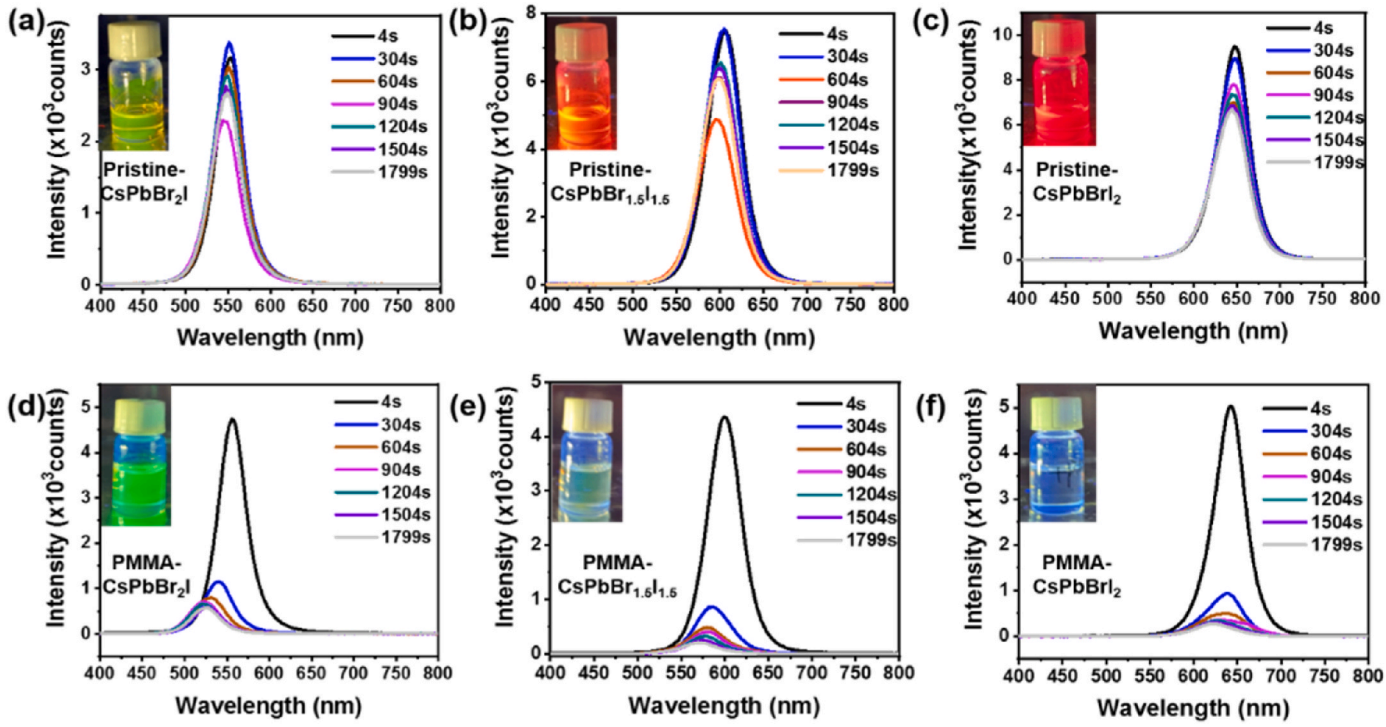

Fig. 2. Temporal evolution of the emission spectra of pristine $CsPbBr_2I$ NCs solution (a), pristine $CsPbBr_{1.5}I_{1.5}$ NCs solution (b) and pristine $CsPbBrI_2$ NCs solution (c) under 450 nm excitation. Temporal evolution of the emission spectra of $CsPbBr_2I$ NCs (d), $CsPbBr_{1.5}I_{1.5}$ NCs (e) and $CsPbBrI_2$ NCs (f) solutions with the addition of PMMA under 450 nm excitation. The inset graphs are colorful pictures corresponding to the $CsPbBr_xI_{3-x}$ NCs solution under UV illumination after 30 min of excitation.

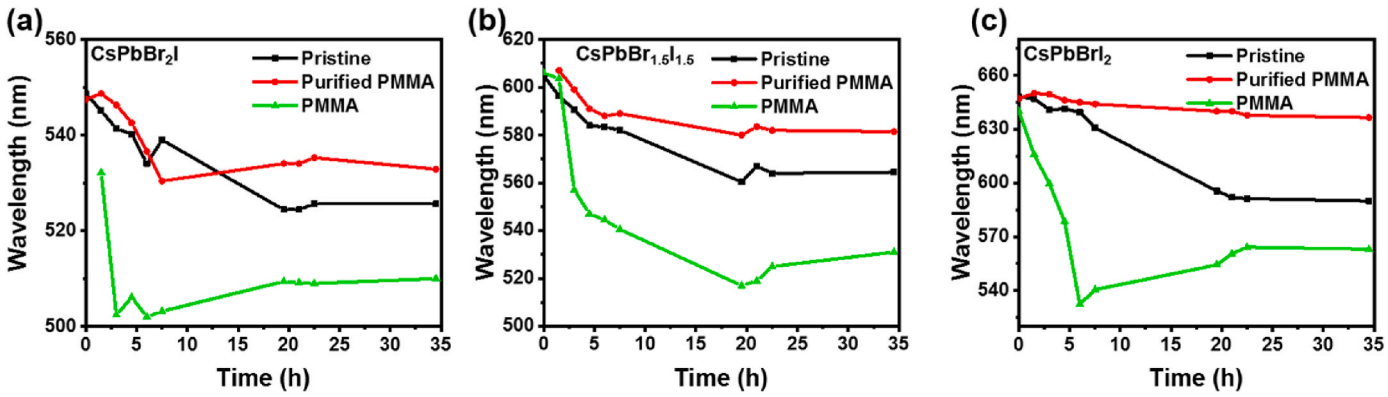

Fig. 3. Temporal evolution of the peak position of the $CsPbBr_2I$ NCs solution (a), $CsPbBr_{1.5}I_{1.5}$ NCs solution (b) and $CsPbBrI_2$ NCs solution (c) which were stored in dark.

Furthermore, the mixed-halide perovskite NCs were also made into films to check if there was any protective effect in the solid-state. Fig. 4, Fig. S1 and Fig. S2 show the PL images of the three kinds of $CsPbBr_xI_{3-x}$ NCs treated under different conditions, in which clear differences can be seen with our naked eyes. The freshly prepared film always showed yellow, orange and red PL for $CsPbBr_2I$, $CsPbBr_{1.5}I_{1.5}$ and $CsPbBrI_2$ NCs (Fig. S1a, Fig. 4a, Fig. S2a), while after 4 days of storage in the dark, the $CsPbBr_xI_{3-x}$ (X = 2, 1.5, 1) NCs embedded in purified PMMA film still maintained a similar color ((Fig. S1c, Fig. 4c, Fig. S2c)), while the pristine $CsPbBr_xI_{3-x}$ NCs without polymer matrix and the $CsPbBr_xI_{3-x}$ NCs embedded in unpurified PMMA almost completely degraded, both of which exhibited green emission, as shown in Fig. 4b, Fig. S1b and Fig. S2b. The unchanged PL spectra of the NCs embedded in purified PMMA shown in Fig. 4f, Fig. S1f and Fig. S2f also proved that purification of PMMA indeed has protection effects on mixed-halide perovskite NCs. Here, the PL shift in films was different from that in solutions (Fig. 3), which can be explained by the $CsPbBr_xI_{3-x}$ NCs solution being in a dynamic equilibrium state. The interactions among the ions, ligands, solutions and ambient atmosphere will become more frequent, leading to the rapid blueshift of the PL. However, the freedom of $CsPbBr_{xI3-x}$ NCs embedded in films is much lower than that in solutions, and the range of the interactions was also limited to $CsPbBr_{xI3-x}$ NCs, polar species in film and ambient atmosphere. Thus, the PL shift of $CsPbBr_xI_{3-x}$ NCs in film will become slower than that in solutions. Furthermore, when comparing pristine $CsPbBr_xI_{3-x}$ NCs solution with that mixed in commercial PMMA solution, although the former exhibited better stability, they still cannot bear the destruction effects from oxygen and moisture when deposited on substrates for a long duration. In addition to the effect of enhanced stability, the polymer matrix (purified PMMA) can also help to fabricate uniform and well distributed luminescent films (Fig. S5), which are required for application in LEDs.

To understand the mechanism of the destructive effects of commercial PMMA, detailed investigations were performed. We first checked the influence of the polymer matrix on the morphology of the $CsPbX_3$ NCs using HRTEM for both commercial and purified PMMA. As shown in Fig. S6, the crystal lattice decreased when embedded in commercial PMMA compared with that in purified PMMA, indicating a reduction in iodine content when embedded in unpurified PMMA, which is consistent with the experimental results presented by the PL spectra. Then, the time-resolved photoluminescence (TRPL) of the three NCs in different media was also characterized, as shown in Fig. 5a–c. The PL decay curves were fitted by a triple-exponential function, and the average lifetimes are presented in Table S1. The PL lifetime in purified PMMA exhibited a slight decrease compared with that in toluene. This should

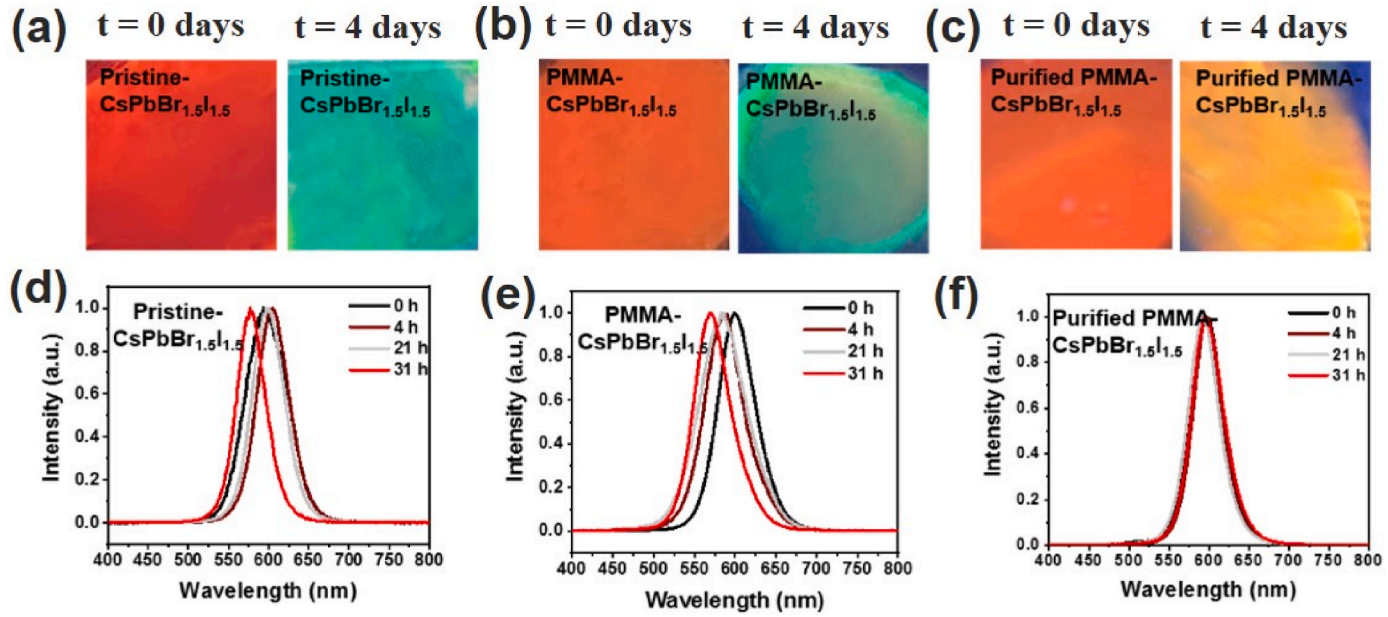

Fig. 4. (a), (b) and (c) Comparison of PL images of the newly prepared $CsPbBr_{1.5}I_{1.5}$ NCs films and $CsPbBr_{1.5}I_{1.5}$ NCs films after 4 days with different polymer matrix conditions. (d), (e) and (f) Corresponding temporal evolution of the emission spectra.

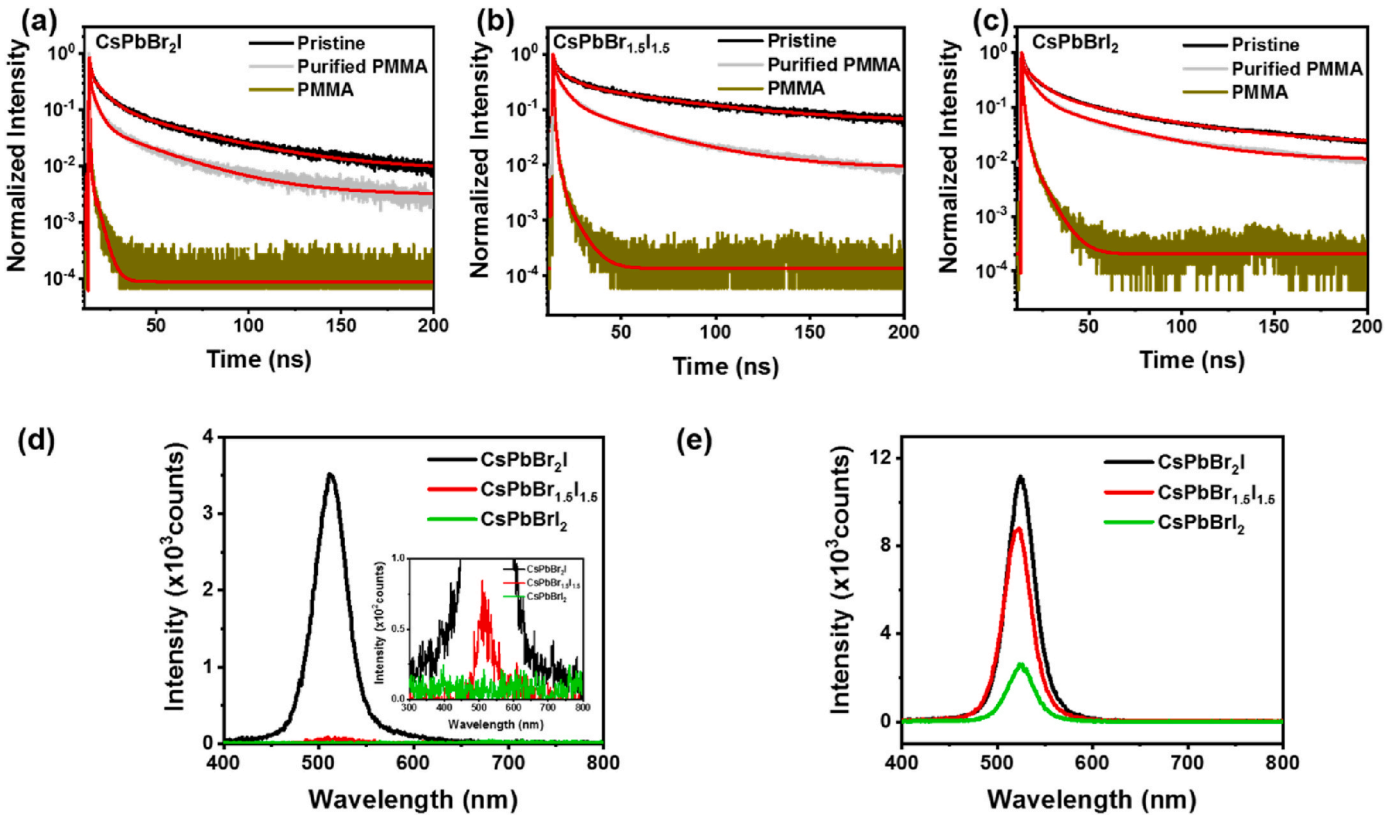

Fig. 5. PL lifetime of $CsPbBr_2I$ NCs (a), $CsPbBr_{1.5}I_{1.5}$ NCs (b) and $CsPbBrI_2$ NCs (c). (d) PL spectra from $CsPbBr_xI_{3-x}$ NCs samples in commercial PMMA after 24 h. (e) PL spectra from $CsPbBr_xI_{3-x}$ NCs samples in acetone after 8 h.

be because the side of the main chain in PMMA contains a methyl ester group, and the polarity is larger than that of toluene, which can produce charge transfer between the exposed surface of $CsPbBr_{xI3-x}$ NCs and PMMA molecules. The PL lifetime of $CsPbBr_xI_{3-x}$ NCs blending in commercial PMMA showed a much faster PL decay than in the other two mediums. Since the PMMA molecules will not lead to such fast PL decay, there must be something with larger polarity than PMMA, which greatly enhances the charge transfer efficiency between the exposed surface of $CsPbBr_{xI3-x}$ NCs and PMMA molecules. Such polar species also cause destructive effects on the surface ligands, which further contribute to the fast PL decay by increasing the exposed surface area of $CsPbBr_xI_{3-x}$ NCs. Because such polar species can be effectively removed by the purification process, we proposed that some polar impurities in the commercial PMMA can interact with the $CsPbBr_xI_{3-x}$ NCs and destroy the surface ligands under light illumination. Such a process will promote the charge transfer efficiency, leading to an obvious reduction in the PL lifetime. Of course, although we mostly ascribe the slight decrease in the PL lifetime to the charge transfer between $CsPbBr_xI_{3-x}$ NCs and PMMA molecules, we still cannot guarantee the 100% elimination of impurities with strong polarity. The residuals in purified PMMA can also contribute to the slight decrease in the lifetime of NCs. In addition, accompanying the destruction of the surface ligands, the NCs could partially dissolve in the solutions, or the organic ammonium was inclined to capture I^- in the NCs, resulting in the structural transformation of the mixed halide perovskite NCs exhibiting a blueshift in the PL emission.

As is well known, conventional synthesis of perovskite NCs will always introduce oleylamine (OLA) as capping ligands and oleic acid (OA) to maintain the stability of the surface ligands. [34] Since the destruction of the OA will break the combination between capping ligands and the surface of NCs, polar species functioning as strong bases could be the most likely candidates. In fact, during the polymerization of PMMA, a radical initiator is needed. These species can always work as initiators for some molecules with strong polarities, e.g., benzoyl peroxide (PhC(O)O)$_2$ (BPO) [35], which should play the main role in the interaction with OA molecules leading to the destruction of equilibrium in solutions. To verify the destructive effects of polar species on capping ligands (OA), by introducing species with different polarities, such as acetone and ethyl acetate, into $CsPbBr_3$ NCs solutions, the redshift of the PL emission can be clearly observed when acetone is added, while the PL spectra in ethyl acetate remained constant, as shown in Fig. S7, indicating the destructive effect on OA of the species with strong polarity, which is consistent with previous reports. [36,37] In addition, we also directly introduced BPO molecules into the $CsPbBr_3$ NCs solutions and observed a slow redshift of the PL emission, which can also verify the destruction effect of BPO on OA ligands. Then, the drop in OLA ligands will accompany the adsorption of I^- on the $CsPbBr_xI_{3-x}$ NCs surface, considering that the larger ionic radius of I^- will weaken the interaction between Pb^{2+} and I^- compared to Br^-. Organic ammonium is more likely to associate with I^-[38], which causes I^- to drop from the surface. In addition, the strong oxidation effect of BPO can also simultaneously contribute to the destruction of iodine ions on $CsPbBr_xI_{3-x}$ NCs due to the larger ionic radius of I^- than Br^-. Thus, with enough interaction time, I^- will be gradually extracted and destroyed, and the PL spectra of all $CsPbBr_xI_{3-x}$ (X = 2, 1.5, 1) NCs will become close. The final PL maxima of $CsPbBr_xI_{3-x}$ NCs blending in unpurified PMMA shown in Fig. 5d were all approximately 520 nm, proving our assumption. Such a mechanism can also be verified from the reported results. Since most investigators mainly used commercial PMMA without purification to protect $MAPbBr_3$ or $CsPbBr_3$ NCs, which were free from iodine contents, from the influences of moisture and oxygen, the PL spectra of the pure-phase perovskite can always remain stable (e.g., ~520 nm for $CsPbBr_3$ NCs). [22,23] As a result, they only observed the protection effects of the polymer matrix (without purification) on pure-phase perovskite NCs and ignored the destructive effects of the polar species in the unpurified matrix on mixed-halide perovskite NCs. Finally, to directly prove that the species with strong polarity and oxidization effects can induce

destructive effects on mixed-halide perovskite NCs, we also first tried to introduce solvent molecules of different polarities into pristine $CsPbBr_xI_{3-x}$ NCs (Fig. S8) and found that only acetone molecules with strong polarity can induce similar variation processes in the PL spectra (Fig. S9) observed in unpurified PMMA. Additionally, as shown in Fig. 5e and d, the final PL spectra of PMMA treated with acetone molecules were also similar to those in unpurified PMMA, which further proved the destructive effect of species with strong polarity. In addition to the polar species, the BPO molecules with oxidation effects as mentioned before were also introduced into the $CsPbBr_xI_{3-x}$ NCs solutions, and a fast blue shift of the PL spectra took place under continuous excitation, as shown in Fig. S10, demonstrating the destruction effect of oxidizing species (e.g., BPO) on mixed-halide perovskite NCs. Therefore, both experimental results of polar and oxidizing species can be a convincing proof for our assumption that commercial PMMA can contain some polar and oxidation impurities that can effectively destroy the mixed-halide perovskite NCs.

4. Conclusions

In summary, we successfully verified the destructive effects of a commercial polymer matrix PMMA on mixed-halide $CsPbBr_xI_{3-x}$ NCs, which limited their applications. Further experiments confirmed that $CsPbBr_xI_{3-x}$ NCs embedded in purified PMMA can exhibit superior stability in both solution and film. Additionally, the destructive effects were investigated due to the synergistic effect of polar and oxidizing species in the commercial polymer matrix, surface ligands and halide ions in $CsPbBr_xI_{3-x}$. As a result, the promoted degradation mechanism and the optimized strategy of the mixed-halide perovskite NCs in media containing polar and oxidizing species will provide guidance for how to better utilize $CsPbBr_xI_{3-x}$ NCs, a promising candidate for optoelectronic devices, to develop colorful light-emitting devices.

Author statement

All authors listed have made significant contribution to the manuscript and reviewed this article. Y. Zhu, D. Hong and Y. Nie: Data curation, investigation and analysis. Y. Zhu and D. Hong: Conceptualization and writing-original draft. H. Liu: TEM characterization. S. Wan, M. Xie, W. Yang, Z. Wei and S. Ye: Discussion, suggestions and reagents providing. D. Hong and Y. Tian: Supervision, editing draft, Project administration and funding acquisition.

Declaration of competing interest

The authors declare that they have no known competing financial interests or personal relationships that could have appeared to influence the work reported in this paper.

Data availability

Data will be made available on request.

Acknowledgements

This work is supported by the National Natural Science Foundation of China (NSFC Nos. 22073046 and 62011530133), the Fundamental Research Funds for the Central Universities (020514380256 and 020514380278), the Double-Innovation Doctor Program of Jiangsu Province, China (No. JSSCBS20211151) and Funding for School-level Research Projects of Yancheng Institute of Technology (xjr2021062).

Appendix A. Supplementary data

Supplementary data to this article can be found online at https://doi.org/10.1016/j.jlumin.2022.119147.

References

[1] J.S. Manser, J.A. Christians, P.V. Kamat, Intriguing optoelectronic properties of metal halide perovskites, Chem. Rev. 116 (2016) 12956–13008.
[2] Y. Cai, Y. Li, L. Wang, R.-J. Xie, A facile synthesis of water-resistant $CsPbBr_3$ perovskite quantum dots loaded poly(methyl methacrylate) composite microspheres based on in situ polymerization, Adv. Opt. Mater. 7 (2019), 1901075.
[3] A. Ray, B. Martín-García, A. Moliterni, N. Casati, K.M. Boopathi, D. Spirito, L. Goldoni, M. Prato, C. Giacobbe, C. Giannini, F. Di Stasio, R. Krahne, L. Manna, A. L. Abdelhady, Mixed dimethylammonium/methylammonium lead halide perovskite crystals for improved structural stability and enhanced photodetection, Adv. Mater. 34 (2022), 2106160.
[4] D.N. Dirin, L. Protesescu, D. Trummer, I.V. Kochetygov, S. Yakunin, F. Krumeich, N.P. Stadie, M.V. Kovalenko, Harnessing defect-tolerance at the nanoscale: highly luminescent lead halide perovskite nanocrystals in mesoporous silica matrixes, Nano Lett. 16 (2016) 5866–5874.
[5] G. Long, C. Jiang, R. Sabatini, Z. Yang, M. Wei, L.N. Quan, Q. Liang, A. Rasmita, M. Askerka, G. Walters, X. Gong, J. Xing, X. Wen, R. Quintero-Bermudez, H. Yuan, G. Xing, X.R. Wang, D. Song, O. Voznyy, M. Zhang, S. Hoogland, W. Gao, Q. Xiong, E.H. Sargent, Spin control in reduced-dimensional chiral perovskites, Nat. Photonics 12 (2018) 528–533.
[6] T. Chen, M. Huang, Z. Ye, J. Hua, S. Lin, L. Wei, L. Xiao, Blinking $CsPbBr_3$ perovskite nanocrystals for the nanoscopic imaging of electrospun nanofibers, Nano Res. 12 (2021) 1397–1404.
[7] P. Ramasamy, D.-H. Lim, B. Kim, S.-H. Lee, M.-S. Lee, J.-S. Lee, All-inorganic cesium lead halide perovskite nanocrystals for photodetector applications, Chem. Commun. 52 (2016) 2067–2070.
[8] J.D. Shi, W.Y. Ge, J.F. Zhu, M. Saruyama, T. Teranishi, Core-shell $CsPbBr_3$@CdS quantum dots with enhanced stability and photoluminescence quantum yields for optoelectronic devices, ACS Appl. Nano Mater. 3 (8) (2020) 7563–7571.
[9] H. Zhang, X. Wang, Q. Liao, Z. Xu, H. Li, L. Zheng, H. Fu, Embedding perovskite nanocrystals into a polymer matrix for tunable luminescence probes in cell imaging, Adv. Funct. Mater. 27 (2017), 1604382.
[10] S. Yang, W. Bao, X.Z. Liu, J.M. Kim, R.K. Zhao, R.M. Ma, Y. Wang, X. Zhang, Subwavelength-scale lasing perovskite with ultrahigh purcell enhancement, Matter 4 (2021) 4042–4050.
[11] R.D. Zhao, Z.K. Gu, P.W. Li, Y.Q. Zhang, Y.L. Song, Flexible and wearable optoelectronic devices based on perovskites, Adv. Mater. Technol. 7 (2021), 2101124.
[12] T. Chiba, Y. Hayashi, H. Ebe, K. Hoshi, J. Sato, S. Sato, Y.-J. Pu, S. Ohisa, J. Kido, Anion-exchange red perovskite quantum dots with ammonium iodine salts for highly efficient light-emitting devices, Nat. Photonics 12 (2018) 681–687.
[13] Y. Kim, E. Yassitepe, O. Voznyy, R. Comin, G. Walters, X. Gong, P. Kanjanaboos, A. F. Nogueira, E.H. Sargent, Efficient luminescence from perovskite quantum dot solids, ACS Appl. Mater. Interfaces 7 (2015) 25007–25013.
[14] Yi, Wei, Hui, Xiao, Zhongxi, Shuang Xie, Liang, Sisi, Liang, Highly luminescent lead halide perovskite quantum dots in hierarchical CaF_2 matrices with enhanced stability as phosphors for white light-emitting diodes, Adv. Opt. Mater. 6 (2018), 1701343.
[15] Y.T. Hsieh, Y.F. Lin, W.R. Liu, Enhancing the water resistance and stability of $CsPbBr_3$ perovskite quantum dots for light-emitting-diode applications through encapsulation in waterproof polymethylsilsesquioxane aerogels, ACS Appl. Mater. Interfaces 12 (2020) 58049–58059.
[16] S.J. Zhao, et al., Geopolymer-encapsulated cesium lead bromide perovskite nanocrystals for potential display applications, ACS Appl. Nano Mater. 3 (2020) 11695–11700.
[17] S. Pathak, N. Sakai, F.W.R. Rivarola, S.D. Stranks, H.J. Snaith, Perovskite crystals for tunable white light emission, Chem. Mater. 27 (2015) 8066–8075.
[18] S.N. Raja, Y. Bekenstein, M.A. Koc, S. Fischer, D. Zhang, L. Lin, R.O. Ritchie, P. Yang, A.P. Alivisatos, Interfaces, encapsulation of perovskite nanocrystals into macroscale polymer matrices: enhanced stability and polarization, ACS Appl. Mater. Interfaces 8 (2016) 35523–35533.
[19] X.B. Tang, N.L. Kothalawala, Y.L. Zhang, D.L. Qian, D.Y. Kim, F.Q. Yang, Water-driven $CsPbBr_3$ nanocrystals and poly(methyl methacrylate)-$CsPbBr_3$ nanocrystal films with bending-endurable photoluminescence, Chem. Eng. J. (2021) 425.
[20] J. Zhu, Z. Xie, X. Sun, S. Zhang, G. Pan, Y. Zhu, B. Dong, X. Bai, H. Zhang, H. Song, Highly efficient and stable inorganic perovskite quantum dots by embedding into a polymer matrix, ChemNanoMat 5 (2019) 346–351.
[21] Y. Xin, H. Zhao, J. Zhang, Highly stable and luminescent perovskite–polymer composites from a convenient and universal strategy, ACS Appl. Mater. Interfaces 10 (2018) 4971–4980.
[22] X. Li, Z. Xue, D. Luo, et al., A stable lead halide perovskite nanocrystals protected by PMMA, Sci. China Mater. 61 (2018) 363–370.
[23] Y. Wang, L. Varadi, A. Trinchi, J. Shen, Y. Zhu, G. Wei, C. Li, Spray-assisted coil–globule transition for scalable preparation of water-resistant $CsPbBr_3$@PMMA perovskite nanospheres with application in live cell imaging, Small 14 (2018), 1803156.
[24] X. Li, Y. Wu, S. Zhang, B. Cai, Y. Gu, J. Song, H. Zeng, $CsPbX_3$ quantum dots for lighting and displays: room-temperature synthesis, photoluminescence superiorities, underlying origins and white light-emitting diodes, Adv. Funct. Mater. 26 (2016) 2435–2445.
[25] W. Dan, W. Dan, D. Di, C. Wei, X. Sun, Polarized emission from $CsPbX_3$ perovskite quantum dots, Nanoscale 8 (2016) 11565–11570.
[26] C. Wang, A.S.R. Chesman, J.J. Jasieniak, Stabilizing the cubic perovskite phase of $CsPbI_3$ nanocrystals by using an alkyl phosphinic acid, Chem. Commun. 53 (2017) 232–235.

[27] X. Li, Y. Wu, S. Zhang, B. Cai, Y. Gu, J. Song, H. Zeng, $CsPbX_3$ quantum dots for lighting and displays: room-temperature synthesis, photoluminescence superiorities, underlying origins and white light-emitting diodes, Adv. Funct. Mater. 26 (2016) 2435–2445.
[28] S. Kango, S. Kalia, A. Celli, J. Njuguna, Y. Habibi, R. Kumar, Surface modification of inorganic nanoparticles for development of organic–inorganic nanocomposites-a review, Prog. Polym. Sci. 38 (2013) 1232–1261.
[29] L. Gao, L.N. Quan, F.P. García de Arquer, et al., Efficient near-infrared light-emitting diodes based on quantum dots in layered perovskite, Nat. Photonics 14 (2020) 227–233.
[30] T. Li, S. He, A. Stein, L.F. Francis, F.S.J.M. Bates, Synergistic toughening of epoxy modified by graphene and block copolymer micelles, Macromolecules 49 (2016) 9507–9520.
[31] S.M. George, B. Yoon, A.A. Dameron, Surface chemistry for molecular layer deposition of organic and hybrid organicinorganic polymers, Acc. Chem. Res. 42 (2009) 498–508.
[32] Dubale, et al., Organometal halide perovskite solar cells: degradation and stability, Energy Environ. Sci. 9 (2016) 323–356.
[33] M. Meyns, et al., Polymer-enhanced stability of inorganic perovskite nanocrystals and their application in color conversion leds, ACS Appl. Mater. Interfaces 8 (2016) 19579–19586.
[34] D. Yang, X. Li, W. Zhou, S. Zhang, H. Zeng, $CsPbBr_3$ quantum dots 2.0: benzenesulfonic acid equivalent ligand awakens complete purification, Adv. Mater. 31 (2019), 1900767.
[35] Y. Tian, V. Sheinin, O. Kulikova, N. Mamardashvili, I.G. Scheblykin, Improving photo-stability of conjugated polymer MEH-PPV embedded in solid matrices by purification of the matrix polymer, Chem. Phys. Lett. 599 (2014) 142–145.
[36] F. Krieg, S.T. Ochsenbein, S. Yakunin, S. ten Brinck, P. Aellen, A. Suess, B. Clerc, D. Guggisberg, O. Nazarenko, Y. Shynkarenko, S. Kumar, C.-J. Shih, I. Infante, M. V. Kovalenko, Colloidal $CsPbX_3$ (X = Cl, Br, I) nanocrystals 2.0: Zwitterionic capping ligands for improved durability and stability, ACS Energy Lett. 3 (2018) 641–646.
[37] Y. Sun, H. Zhang, K. Zhu, W. Ye, L. She, X. Gao, W. Ji, Q. Zeng, Research on the influence of polar solvents on $CsPbBr_3$ perovskite QDs, RSC Adv. 11 (2021) 27333–27337.
[38] Q.A. Akkerman, V. D' Innocenzo, S. Accornero, A. Scarpellini, A. Petrozza, M. Prato, L. Manna, Tuning the optical properties of cesium lead halide perovskite nanocrystals by anion exchange reactions, J. Am. Chem. Soc. 137 (2015) 10276–10281.